

Diffusion of dark matter in a hot and dense nuclear environmentMarina Cermeño,^{1,*} M. Ángeles Pérez-García,^{1,†} and Joseph Silk^{2,3,4,‡}¹*Department of Fundamental Physics, University of Salamanca,
Plaza de la Merced s/n 37008 Salamanca, Spain*²*Institut d'Astrophysique, UMR 7095 CNRS, Université Pierre et Marie Curie,
98bis Boulevard Arago, 75014 Paris, France*³*Department of Physics and Astronomy, The Johns Hopkins University,
Homewood Campus, Baltimore, Maryland 21218, USA*⁴*Beecroft Institute of Particle Astrophysics and Cosmology, Department of Physics, University of Oxford,
Oxford OX1 3RH, United Kingdom*

(Received 12 November 2015; revised manuscript received 20 May 2016; published 7 July 2016)

We calculate the mean free path in a hot and dense nuclear environment for a fermionic dark matter particle candidate in the \sim GeV mass range interacting with nucleons via scalar and vector effective couplings. We focus on the effects of density and temperature in the nuclear medium in order to evaluate the importance of the final state blocking in the scattering process. We discuss qualitatively possible implications for opacities in stellar nuclear scenarios, where dark matter may be gravitationally accreted.

DOI: 10.1103/PhysRevD.94.023509

I. INTRODUCTION

There are multiple indications pointing toward a model containing cold dark matter (DM) as the best explanation for the universe we see at different scales. In particular, the importance of the dark sector component of matter on stellar scales has been less extensively studied and has mainly focused on the sun, planets, white dwarfs [1–3], and compact stars [4]. This is due to the expected moderate capability of gravitational accretion by these individual celestial bodies from an existing DM galactic distribution. Although the current situation of DM searches has greatly benefited from a world-wide experimental effort, at the present time, there still remains a relatively vast DM phase space to explore. Regarding possible values for DM particle masses within the weak interaction sector (*wimp* scenario), most popular candidates range from the sub-GeV region up to \sim 100 TeV. As for the interaction cross sections with nuclear matter (i.e., nucleons, N), there are at least five orders of magnitude in the \sim GeV mass range remaining to be fully tested, namely, $\sigma_{\chi N} \sim 10^{-43}$ – 10^{-48} cm² as quoted by direct detection searches [5].

Apart from this, concerning the nature of the DM particle, in the case of a Majorana candidate, the expected indirect signal involving gamma rays or neutrino final products is still under debate [6]. In this same direction, we may cite other astrophysical effects such as the modification of the emissivity of Standard Model neutrinos from solar reaction chains that have been recently suggested [7]. In the case of asymmetric candidates, accretion of DM mass beyond a critical value, i.e., the Chandrasekhar mass,

could induce a dramatic fate for the star where DM accumulates over time [8–10] and eventually collapses to a black hole. Another catastrophic event could be triggered following compact object formation via DM seeding. In case of a Majorana candidate, it could induce spark formation energetic enough to nucleate stable bubbles of deconfined quark matter leading to a softening of the nucleon equation of state. This would drive a neutron star to quark star conversion [11–13]. In addition, unstable DM can also be constrained by structural stability of accreting objects [14].

However, aside from a pure particle physics description, from the thermodynamical point of view, average magnitudes incorporating the effect of a novel dark sector could be, in principle, determined by evaluating the interplay of both types of matter in a common environment. Typically, the possible dark self-interaction effects are expected to be small as long as the numbers of DM particles remain tiny at all times, with respect to the baryons, and their relative fraction $Y_\chi = N_\chi/N_B \ll 1$. This could be important, however, for a precise determination of the critical dark matter mass capable of being sustained in a star [8].

As mentioned before, for a given candidate, $\sigma_{\chi N}$ mainly determines the relative fraction of DM to be captured by a compact-sized (spherical) object of mass M and radius R . Once inside, it is believed to diffuse toward the denser central stellar regions according to the exponential law $\sim e^{-m_\chi \phi(r)/k_B T(r)}$, being $T(r)$ a local temperature, $\phi(r)$ the gravitational potential and r the radial coordinate [15].

As an order-of-magnitude estimate, the mean free path of a DM particle, λ_χ , is quoted as $\lambda_\chi \simeq 1/\sigma_{\chi N} n$, where n is the ordinary nucleon number density. This is usually considered as being sufficient to obtain knowledge about the most

*marinacgavilan@usal.es

†mperezga@usal.es

‡silk@iap.fr

efficient opaque environments. For example, a dense nuclear medium such as the central core in a neutron star (with a content $\gtrsim 90\%$ neutrons) exhibits densities well in excess nuclear saturation density $n_0 \approx 0.17 \text{ fm}^{-3}$. It is important to note, however, that in-medium effects are mostly absent from the previous rough estimate. Let us briefly comment on some of the missing corrections. To begin with, Fermi blocking due to partial restriction of the outgoing nucleon phase space can play a role diminishing the χN cross section. Finite temperature effects will additionally allow the population of higher energy states in the nucleon sector with respect to the vanishing temperature case to provide the opposite effect. Let us remind ourselves here that temperatures in the range of $T \lesssim 50 \text{ MeV}$ are usually achieved in the very early stages of proto-neutron star evolution [16]. Later, after a primary neutrino cooling era, temperatures fall to the $\sim \text{keV}$ range. This will effectively set at large times a $T \approx 0$ configuration, as thermal energies are indeed much smaller than nucleon Fermi energies $k_B T \ll E_{FN}$ in the dense medium.

Motivated for the need to compare bounds from the colliders to direct detection, one can describe interactions between DM and fermions with effective operators in the context of effective field theories (EFT). In direct detection searches, for example, a nonrelativistic incoming χ particle with low Maxwellian velocity, $v/c \ll 1$, is considered. However, collider searches can constrain the high energy part of the interaction as particles are increasingly more relativistic $v/c \sim 1$ allowing, in addition, higher values of \sqrt{s} and momentum transfer $\sim \text{TeV}$. Typically, all the quoted interactions have been largely explored in very low density or vacuum conditions. In particular, scalar, vector, and pseudoscalar couplings can play a crucial role as seen in [17,18]. To test increasing relativistic velocity ranges, natural sources of acceleration can be provided by gravitational boosting near compact stars. In this way, (neutral) DM particles can acquire large velocities $v \sim c$ and scatter very dense macroscopic regions of size nearly the radius of the star $R \sim 10\text{--}12 \text{ km}$. This extent has so far only been marginally explored [19,20]. In this work, we focus on the impact of the relativistic contribution of scalar and vector χN couplings to the spin-independent (SI) diffusion of DM inside a dense and hot nuclear medium.

The structure of this contribution is as follows. In Sec. II, we present the effective field theory Lagrangian model using dark matter-nucleon contact interaction via scalar and vector couplings in a relativistic framework. Later, we compute the doubly differential and integrated χN cross sections at finite nucleon chemical potential and temperature. We especially focus on the resulting diffusive behavior of weakly interacting DM particles. In Sec. III, we discuss the obtained dependencies by presenting the figures for selected cases. Finally, in Sec. IV, we give our conclusions.

II. DARK MATTER MODEL AND CROSS SECTIONS

We consider a fermionic dark matter particle of Dirac type, χ , with scalar and vector couplings to the nucleon field N (protons and neutrons). We can write the interaction Lagrangian under the form

$$\mathcal{L}_{\mathcal{I}} = \sum_{N=n,p} g_{Ns} \chi \bar{\chi} N \bar{N} + g_{Nv} \chi \gamma^\mu \bar{\chi} N \gamma_\mu \bar{N}, \quad (1)$$

where γ_μ are the Dirac matrices and g_{Ns}, g_{Nv} are the scalar and vector coupling constants, respectively. This treatment is already used in direct detection at low energies with nonrelativistic effective field theory operators as shown in [21]. Typically, elastic scattering (rather than inelastic) is considered as it is the case relevant for direct detection. Generically, operators containing two fermionic dark matter fields can be categorized as shown in [5,22]. In particular, we focus on those labeled D1 and D5, both contributing to the SI interaction. This interaction is equivalent to considering a Fermi four-fermion interaction model, where the effective couplings of mass dimension (-2) for these operators are obtained by integrating out the propagator of a generic ϕ mediator with mass M_ϕ . Motivated by the need to compare bounds from colliders to direct detection, we describe interactions of DM with quarks $q = u, d$, and averaging in terms of nucleon fields, we can write for the vector case $g_{Nv}/M_\phi^2 \sim 1/\Lambda_v^2$ and $g_{Ns}/M_\phi^2 \sim m_q/\Lambda_s^3$, where Λ_v (Λ_s) is the suppression mass scale for the vector (scalar) case. As usual, we are assuming the effective couplings are of order $O(1)$ and can be absorbed into $\Lambda_{s,v}$ [23]. Using bounds from CMS and ATLAS [24,25], we set $\Lambda_v \gtrsim 1 \text{ TeV}$ and $\Lambda_s \gtrsim 100 \text{ GeV}$. At this point, it is worth mentioning that a larger parameter range can be considered by means of a multiplicative factor in each coupling, g_{Ns}, g_{Nv} . We have selected these values as they refer to families of phenomenological models that are currently allowed.

Usually, the incoming DM particle is supposed to be thermalized in the galaxy with the Maxwellian mean velocities $\bar{v} \sim 220 \text{ km/s}$. However, in the scenario we consider, an accreting dense star (typically with the mass and dimensions of a neutron star), general relativistic effects are non-negligible and are capable of providing a sizable gravitational boost to the incoming DM particle [19,26]. Let us consider, in order to be concrete, a canonical neutron star of mass $M_{\text{NS}} \approx 1.5 M_\odot$ and radius $R_{\text{NS}} \approx 12 \text{ km}$. Expliciting the ratio used as unity, $\frac{GM_{\text{NS}}}{c^2} = 1$, the velocity modulus v at the star surface is given by

$$\beta = \frac{v}{c} = \sqrt{\frac{2GM_{\text{NS}}}{rc^2}} \approx 0.6 \sqrt{\left(\frac{12 \text{ km}}{R_{\text{NS}}}\right) \left(\frac{M_{\text{NS}}}{1.5 M_\odot}\right)}, \quad (2)$$

yielding a minimum Lorentz factor at the surface $\gamma = 1/\sqrt{1-\beta^2} \approx 1.26$. If scattering happens well inside the core, the previous value is a lower limit, then $\gamma \gtrsim 1.26$. The associated wavelength of the incoming DM particle is $\lambda = \frac{2\pi\hbar c}{\sqrt{\gamma^2-1}m_\chi c^2}$. This expression sets, in practice, a measure of the validity of our calculation since matter is tested to sizes around $\lambda \sim 1$ fm, i.e., in the DM mass range $m_\chi \lesssim 5$ GeV. Although further modeling would be required for the description of the inner hadron structure, the use of nuclear form factors can somewhat mitigate the short-range correlations arising in our calculation as we see later in the manuscript.

In order to calculate the differential cross section per unit volume for the DM-nucleon scattering, we use the interaction terms appearing in Eq. (1). We denote $p'^\mu = (E', \vec{p}')$ and $p^\mu = (E, \vec{p})$ as the four-momentum for the outgoing and incoming nucleon of effective mass m_N^* , respectively, and $k'^\mu = (\omega', \vec{k}')$ and $k^\mu = (\omega, \vec{k})$ analogous for the DM particle of mass m_χ . Momentum transfer is denoted by $q^\mu = p'^\mu - p^\mu = k^\mu - k'^\mu$. In this way, $q_0 = E' - E = \omega - \omega'$ and $\vec{q} = \vec{p}' - \vec{p} = \vec{k} - \vec{k}'$. The general expression can be written as [27,28]

$$d\sigma = \frac{|\overline{\mathcal{M}}_N|^2}{4\sqrt{(pk)^2 - m_N^{*2}m_\chi^2}} d\Phi(p, p', k, k') \mathcal{F}_{\mathcal{FB}}, \quad (3)$$

where the phase space volume element is

$$d\Phi(p, p', k, k') = (2\pi)^4 \delta^{(4)}(p + k - p' - k') \frac{d^3\vec{p}'}{(2\pi)^3 2E'} \frac{d^3\vec{k}'}{(2\pi)^3 2\omega'}. \quad (4)$$

Here, $|\overline{\mathcal{M}}_N|^2$ is the square of the scattering amplitude of the process considered in our interaction model that we discuss in detail later. The four-dimensional delta assures the conservation of momentum and energy in the collision. The factor $\mathcal{F}_{\mathcal{FB}}$ accounts for the Fermi blocking term that takes into account the occupation of states and in our calculation affects only to the nucleon sector (protons or neutrons) $\mathcal{F}_{\mathcal{FB}} = f_N(E)(1 - f_N(E'))$ with $f_i(E) = \frac{1}{1 + e^{(E - \mu_i^*)/k_B T}}$ $i = p, n$. Also, μ_i^* is the effective nucleon chemical potential for a particle with isospin of i -type. From this point and in what follows, we consider $\hbar = c = 1$. Let us remark that for the dark sector we assume that all outgoing DM particles states are, in principle, allowed and $1 - f_\chi(\omega') \approx 1$ since the fraction of DM inside the star remains tiny at all times. The validity of this approximation is given by the estimate of DM particles inside the object as $N_\chi(t) \approx N_{0\chi} + C_\chi \delta t$. Using $C_\chi \approx 6 \times 10^{25} \left(\frac{M}{1.5M_\odot}\right) \left(\frac{R}{12 \text{ km}}\right) (m_\chi) \left(\frac{\rho_\chi^{\text{ambient}}}{0.3 \frac{\text{GeV}}{\text{cm}^3}}\right) \left(\frac{\sigma_{\chi N}}{\sigma_0}\right) \text{ s}^{-1}$ [8] and

the number of nucleons in the star $N_N = N_B \approx 10^{58}$, we obtain $Y_\chi = N_\chi/N_N < 10^{-20}$ for an old neutron star with a lifetime $\delta t \sim 10^6$ yr. We assume a cross section $\sigma_{\chi N} > \sigma_0$ larger than the geometrical or critical cross section [2] $\sigma_0 \approx \pi R_{\text{NS}}^2 m_N/M_{\text{NS}} \sim 10^{-45} \text{ cm}^2$ so the star can effectively scatter and capture DM. Let us mention here that the cross section ratio $\sigma_{\chi N}/\sigma_0$ could be, in principle, even smaller than unity, but in that case, the scattering scenario we present would be mostly insensitive to dark matter, assuming cross sections compatible with the range of currently allowed experimental constraints, $\sigma_{\chi N}/\sigma_0 > 1$, however. DM population in the NS (after the supernova explosion) should not be negligible since the massive progenitor $8 M_\odot \lesssim M_{\text{progenitor}} \lesssim 15 M_\odot$ can be efficient in the DM accretion process [14]. Then, $N_{0\chi} \lesssim 10^{39}$ for an environment with ambient DM density $\rho_\chi^{\text{ambient}} \approx 0.3 \text{ GeV/cm}^3$. Effective values of nucleon mass and chemical potential define the *quasi-particle* nature of the nucleon in the medium and differ from the nude values by the presence of average meson fields. In this work, we consider this correction as obtained in the existing literature and refer for further reading to [29].

Since we are interested in calculating the DM particle mean free path, we also consider the differential and integrated cross section *per unit volume*, and thus, we must integrate over the incoming nucleon phase space [27]. Then, our expression reads

$$\frac{d\sigma(\omega)}{V} = \frac{1}{(2\pi)^5} \int d^3\vec{p} \int d^3\vec{k}' \delta(E + \omega - E - \omega') \times \frac{|\overline{\mathcal{M}}_N|^2}{16\omega'E' \sqrt{E^2\omega^2 - m_N^{*2}m_\chi^2}} \mathcal{F}_{\mathcal{FB}}, \quad (5)$$

where we have performed a partial integration over three-dimensional momentum space. The flux expression appearing in the denominator in Eq. (5) as well as the scattering amplitude we discuss later in the manuscript have, in general, momentum dependences. In the cross-section calculation, we have retained only the lowest order terms following [27] since $v_\chi^2 \sim v_N^2 \ll 1$ given $\frac{|\vec{p}_i|}{E_i} = v_i$, $i = \chi, N$ from reference values $v_\chi \sim 0.6$, and nucleon Fermi velocities $v_N \sim v_{FN} = |\vec{p}_{FN}|/E_{FN} \sim 0.4$ at $n = \frac{|\vec{p}_{FN}|^3}{3\pi^2} = n_0$. In particular, for the flux, this leads to the final expression $\sqrt{(pk)^2 - m_N^2 m_\chi^2} = \sqrt{(E\omega - \vec{p}\vec{k})^2 - m_N^2 m_\chi^2} \approx \sqrt{E^2\omega^2 - m_N^2 m_\chi^2}$.

Let us further rewrite Eq. (5) using a dispersion angle θ for the outgoing DM particle. In this way, we obtain $d^3\vec{k}' = |\vec{k}'|^2 2\pi d(\cos\theta) d|\vec{k}'| = 2\pi |\vec{q}| \frac{\omega'}{|\vec{k}'|} d|\vec{q}| dq_0$. This follows from $\omega' d\omega' = |\vec{k}'| d|\vec{k}'|$ and $d(\cos\theta) = \frac{|\vec{q}| d|\vec{q}|}{|\vec{k}'||\vec{q}'|}$. Finally, we obtain after a trivial partial integration,

$$\frac{d\sigma(\omega)}{V} = \frac{1}{(2\pi)^4} \int d^3\vec{p} \int d|\vec{q}| \int dq_0 \delta(q_0 + E - E') \times \frac{|\vec{q}|}{|\vec{k}|} \frac{|\overline{\mathcal{M}}_N|^2}{16E' \sqrt{E^2 \omega^2 - m_N^{*2} m_\chi^2}} \mathcal{F}_{FB}. \quad (6)$$

In this calculation, we restrict ourselves to temperatures and densities typical for the thermodynamical evolution of the stellar core region, that is, $T \lesssim 50$ MeV and $n \simeq (1-3)n_0$. Due to the fact that squared Fermi nucleon velocities are $v_{FN}^2 \ll 1$, we perform an expansion of the single particle energies for the incoming and outgoing nucleon states

$$E = m_N^* + \frac{|\vec{p}|^2}{2m_N^*}, \quad E' = m_N^* + \frac{|\vec{q} + \vec{p}|^2}{2m_N^*}. \quad (7)$$

In order to perform the integral in Eq. (6), we express the energy delta function as

$$\delta(q_0 + E - E') = \frac{m_N^*}{|\vec{p}||\vec{q}|} \delta(\cos\theta - \cos\theta_0) \Theta(|\vec{p}|^2 - |\vec{p}_-|^2), \quad (8)$$

where

$$\cos\theta_0 = \frac{m_N^*}{|\vec{p}||\vec{q}|} \left(q_0 - \frac{|\vec{q}|^2}{2m_N^*} \right), \quad (9)$$

and

$$|\vec{p}_-|^2 = \frac{m_N^{*2}}{|\vec{q}|^2} \left(q_0 - \frac{|\vec{q}|^2}{2m_N^*} \right)^2. \quad (10)$$

Let us now discuss the range of the integration variables. For the energy transfer range $-\infty < q_0 < \omega - m_\chi$ since $m_\chi < \omega' < \infty$ and $|\vec{k}| - |\vec{k}'| < |\vec{q}| < |\vec{k}| + |\vec{k}'|$ from the constraint of a real-valued angle. Instead, at $T = 0$, the energy transfer cannot be negative, so that $q_0 > 0$ and $0 < q_0 < \omega - m_\chi$, and for the incoming nucleon, it follows $|\vec{p}_-| < |\vec{p}| < \infty$. Note that for $T = 0$ in the limit of vanishing kinetic energy for the incoming DM particle, the q_0 range reduces to zero as the outgoing states are all occupied, therefore providing a null cross section, while this is not true in the finite T case as more channels are available.

Finally, if we are interested in the doubly differential cross section, this can be obtained as

$$\frac{1}{V} \frac{d\sigma}{d\Omega dq_0} = \frac{1}{(2\pi)^4} \int_{|\vec{p}_-|}^{\infty} \frac{d|\vec{p}||\vec{p}|}{4E'} \frac{m_N^* |\vec{k}'|}{|\vec{q}|} \delta(\cos\theta - \cos\theta_0) \times \Theta(|\vec{p}|^2 - |\vec{p}_-|^2) \mathcal{M}, \quad (11)$$

with

$$\mathcal{M} = \frac{|\overline{\mathcal{M}}_N|^2 f_N(E)(1 - f_N(E'))}{4\sqrt{E^2 \omega^2 - m_N^{*2} m_\chi^2}}. \quad (12)$$

The sum of scalar(s) and vector(v) contributions from the Lagrangian in Eq. (1) gives a scattering amplitude $\mathcal{M}_N = \mathcal{M}_s + \mathcal{M}_v$, and therefore,

$$|\overline{\mathcal{M}}_N|^2 = \frac{1}{4} \sum_{\text{spins}} \mathcal{M}_N \mathcal{M}_N^* = |\overline{\mathcal{M}}_s|^2 + |\overline{\mathcal{M}}_v|^2 + \frac{1}{2} \sum_{\text{spins}} \mathcal{M}_s^* \mathcal{M}_v, \quad (13)$$

where

$$\begin{aligned} |\overline{\mathcal{M}}_s|^2 &= 4g_{Ns}^2 (p'p + m_N^{*2})(k'k + m_\chi^2), \\ |\overline{\mathcal{M}}_v|^2 &= 8g_{Nv}^2 [2m_N^{*2} m_\chi^2 - m_N^{*2} k'k - m_\chi^2 p'p \\ &\quad + (p'k')(pk) + (p'k)(pk')], \end{aligned}$$

and

$$\frac{1}{2} \sum_{\text{spins}} \mathcal{M}_s^* \mathcal{M}_v = 8g_{Ns} g_{Nv} m_N^* m_\chi (pk + pk' + p'k + p'k').$$

As a further correction at short ranges, we can model the structure of the nucleon with a form factor $F(|\vec{q}|)$. We consider a monopolar form with a cutoff parameter $\Lambda = 1.5$ GeV. Then, we replace $g_{Ns} \rightarrow g_{Ns} F(|\vec{q}|^2)$ and $g_{Nv} \rightarrow g_{Nv} F(|\vec{q}|^2)$ with $F(|\vec{q}|^2) = \frac{\Lambda^2}{\Lambda^2 + q^2}$ so that $F(0) = 1$.

Retaining the lowest order in particle velocities in the averaged squared matrix element, we obtain

$$\begin{aligned} |\overline{\mathcal{M}}_N|^2 &\simeq 4g_{Ns}^2 (E'E + m_N^{*2})(\omega'\omega + m_\chi^2) \\ &\quad + 8g_{Nv}^2 (2m_N^{*2} m_\chi^2 - m_N^{*2} \omega\omega' - m_\chi^2 E'E + 2E'\omega'E\omega) \\ &\quad + 8g_{Ns} g_{Nv} m_N^* m_\chi (E\omega + E\omega' + E'\omega + E'\omega'). \end{aligned}$$

Let us note that if finite temperature is considered detailed balance factors must be added to the medium response to weak probes [30,31] under the form

$$S(q_0, T) = \frac{1}{1 - e^{-\frac{|q_0|}{k_B T}}}. \quad (14)$$

This factor provides the relation between the dynamical nuclear structure factor for positive and negative energy transfers q_0 as the thermodynamic environment can donate energy to the outgoing particle.

As we are interested in obtaining the total integrated cross section per unit volume $\frac{\sigma(\omega)}{V}$ and the inverse of it, i.e., the mean free path, $\lambda_\chi = (\frac{\sigma(\omega)}{V})^{-1}$, we must integrate over all

possible outgoing energy transfer values and solid angle. In this way, we obtain

$$\lambda_\chi^{-1} = \frac{\sigma(\omega)}{V} = \frac{m_N^*}{4(2\pi)^3} \int_0^{\omega-m_\chi} dq_0 \int_{|\vec{k}|-|\vec{k}'|}^{|\vec{k}|+|\vec{k}'|} d|\vec{q}| \times \int_{|\vec{p}-1}^\infty d|\vec{p}| \frac{|\mathcal{M}_N|^2 |\vec{p}| f_N(E)(1-f_N(E')) S(q_0, T)}{4E' |\vec{k}| \sqrt{E^2 \omega^2 - m_N^{*2} m_\chi^2}}. \quad (15)$$

III. RESULTS

In this section, we present the results. We start by discussing the low T regime. We set $g_{N_s} \sim 10^{-15} \text{ MeV}^{-2}$ and $g_{N_v} \sim 10^{-13} \text{ MeV}^{-2}$ and a cutoff parameter $\Lambda = 1.5 \text{ GeV}$. In order to include the effect of the medium, we replace vacuum nucleon mass and chemical potential values by the effective ones at each baryonic density and T [29]. The i th-type isospin is obtained according to $n_i = \frac{2}{(2\pi)^3} \int_0^\infty \frac{4\pi p^2 dp}{1+e^{(\sqrt{p^2+m_N^{*2}}-\mu_i^*)/k_B T}}$.

In Fig. 1, we show the differential cross section per unit volume as a function of the energy transfer q_0 for different values of $|\vec{q}| = 20, 41, 207,$ and 290 MeV with dash-dotted, dashed, dotted, and solid lines, respectively, for a pure neutron system with $n = n_0$. We use $m_\chi = 0.5 \text{ GeV}$ setting $T = 0$. The limiting upper value of the energy transfer is $\omega - m_\chi \approx 130 \text{ MeV}$. The triangular shape is due to the Heaviside Fermi distribution at $T = 0$. Beyond q_0 values limited by real-valued angles in Eq. (9), the scattered states are not allowed since it is kinematically impossible to scatter a nucleon due to lack of empty states.

In Fig. 2, we show the differential cross section per unit volume as a function of the energy transfer q_0 for different values of the nucleon number density $n = (0.5, 1, 2)n_0$ with dotted, dashed, and solid lines, respectively, for

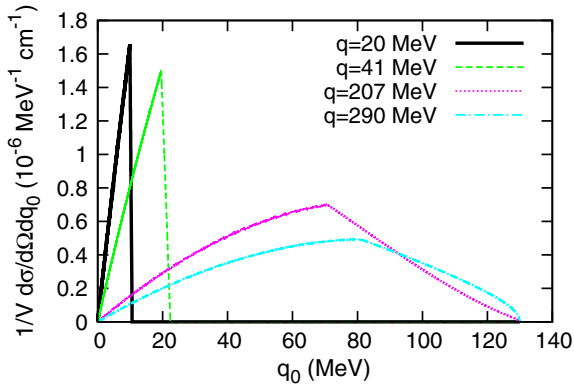


FIG. 1. Differential cross section per unit volume as a function of the energy transfer q_0 for values of $|\vec{q}| = 20, 41, 207,$ and 290 MeV . The DM particle mass is $m_\chi = 0.5 \text{ GeV}$, and $T = 0$ at $n = n_0$.

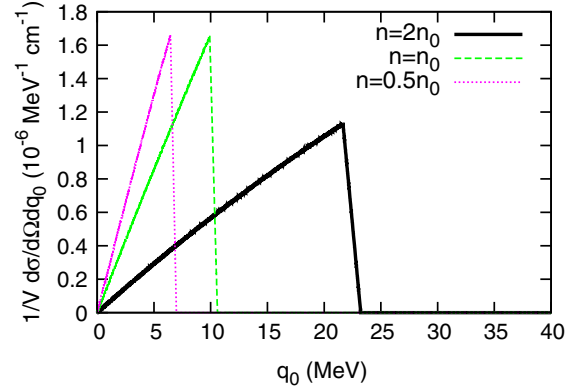


FIG. 2. Differential cross section per unit volume as a function of the energy transfer q_0 for nucleon densities $n = (0.5, 1, 2)n_0$. We set $|\vec{q}| = 20 \text{ MeV}$ and $m_\chi = 0.5 \text{ GeV}$ at $T = 0$.

$|\vec{q}| = 20 \text{ MeV}$. We use $m_\chi = 0.5 \text{ GeV}$ setting $T = 0$ and effective nucleon masses $m_N^*/m_N \approx 0.85, 0.7$ and 0.4 for the increasing density set. A combined effect of the density dependence of nucleon masses and the nucleon Fermi momentum value provide a rapid increase in the maximum q_0 value.

In order to test the variability with the dark probe mass, we depict in Fig. 3 the differential cross section per unit volume as a function of q_0 for mass values $m_\chi = 0.5, 1,$ and 5 GeV . We set $T = 0$ and $n = n_0$ at $|\vec{q}| = 20 \text{ MeV}$. The curve with $m_\chi = 5 \text{ GeV}$ has been decreased by a factor of 10 to make the trend more clear.

Finite temperature effects can be observed in Fig. 4, where the detailed balance factors have been included. We use values of temperature $T = 0, 5,$ and 10 MeV with solid, dashed, and dotted lines, respectively, for $|\vec{q}| = 20 \text{ MeV}$. We set a fixed value of the chemical potential $\mu = E_{FN}$ at $n = n_{\text{sat}}$. This corresponds to densities $n = 0.170, 0.174,$ and 0.209 fm^{-3} setting $m_\chi = 0.5 \text{ GeV}$. At temperatures

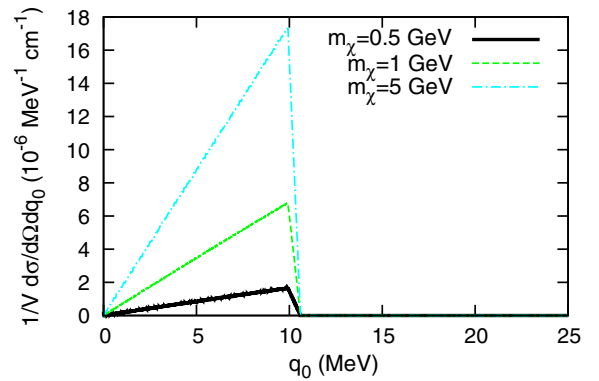


FIG. 3. Differential cross section per unit volume as a function of the energy transfer q_0 for a nucleon density $n = n_0$. We set $|\vec{q}| = 20 \text{ MeV}$ at $T = 0$. The $m_\chi = 5 \text{ GeV}$ case has been decreased by a factor of 10 in this plot.

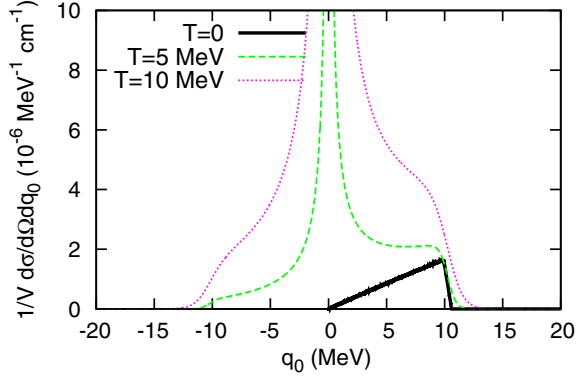


FIG. 4. Differential cross section per unit volume as a function of the energy transfer q_0 at $T = 0, 5, 10$ MeV for a nucleon density $n = n_0$. We set $|\vec{q}| = 20$ MeV and $m_\chi = 0.5$ GeV.

$T > 0$, the negative energy transfer states get increasingly populated, and the sharp nucleon distribution is smoothed. As $q_0 \rightarrow 0$, the inverse detailed balance factor $S^{-1}(q_0, T) \rightarrow 0$. The corresponding divergence will, however, be integrable in order to obtain a finite integrated cross section.

In Fig. 5, we show the mean free path for the χ particle as a function of kinetic energy $K = \omega - m_\chi$ for three mass values $m_\chi = 0.5, 1, \text{ and } 5$ GeV with solid, dashed, and dotted lines, respectively. We set $n = n_0$ and $T = 0$. We can see that in this DM mass range scattering is diffusive to very good approximation as $\lambda/R \ll 1$. We show with the dot-dashed line that the simplified estimate yields a constant value $\lambda_\chi \approx 1/\sigma_{\chi N} n \sim 5.9$ m, assuming sensitivities $\sigma_{\chi N} \sim 10^{-41}$ cm². For our choice of couplings strengths, fixed K energy, a Standard Model neutrino displays typical mean free path somewhat smaller [27,30,32], however, being an efficient heat carrier inside the star. The larger the mass of the DM particle the more opaque is the medium to

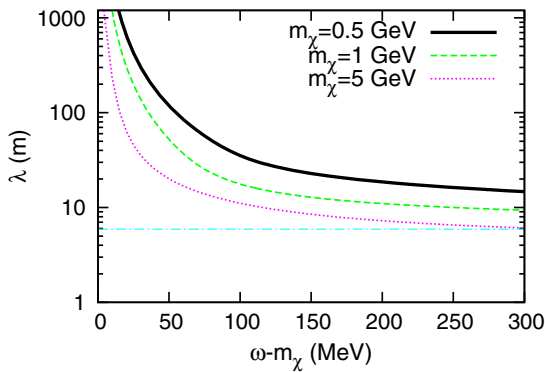


FIG. 5. Dark matter mean free path as a function of kinetic energy for $m_\chi = 0.5, 1, \text{ and } 5$ GeV at $T = 0$ and $n = n_{\text{sat}}$. Dot-dashed line shows that the simplified estimate yields a constant value $\lambda_\chi \approx 1/\sigma_{\chi N} n \sim 5.9$ m, assuming current experimental sensitivities $\sigma_{\chi N} \sim 10^{-41}$ cm². See text for details.

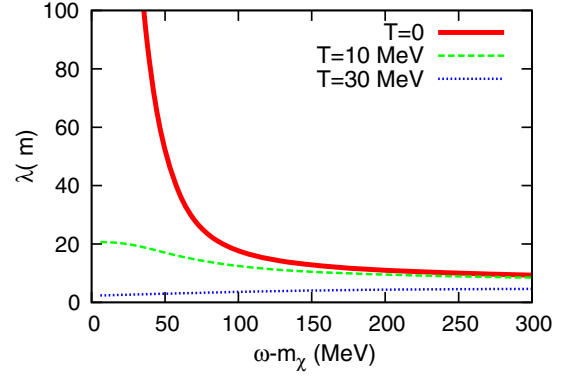


FIG. 6. DM particle mean free path as a function of kinetic energy for $m_\chi = 1$ GeV at $n = n_0$ for $T = 0, 10, \text{ and } 30$ MeV.

it. Note that as $\omega \rightarrow m_\chi$ the phase space available for the outgoing particles vanishes as the energy transferred $q_0 \rightarrow 0$. As all the outgoing states are all occupied in the nucleon sea at $T = 0$, this provides a null value of the integrated cross-section value for the DM-nucleon interaction. This behavior is shown in Fig. 6, where we plot the variation of the mean free path with kinetic energies for temperatures $T = 0$ (solid line), $T = 10$ MeV (dashed line), and $T = 30$ MeV (dotted line). We consider $m_\chi = 1$ GeV and $n = n_0$. At $T = 0$ and vanishing kinetic energy, the mean free path goes arbitrary large as the integrated cross section also vanishes due to filled population levels. This behavior is smoothed at finite temperature, where a nonvanishing mean free path value is recovered.

In Fig. 7, the variation of the DM particle mean free path is shown as a function of density (in units of n_0) for two values of temperature, $T = 0$ (solid line) and $T = 10$ MeV (dashed line). We use $m_\chi = 1$ GeV, and effective nucleon masses have been considered for the $T = 0$ case, while not for the finite temperature case in order to estimate competitive effects. A steady decrease is obtained in case the

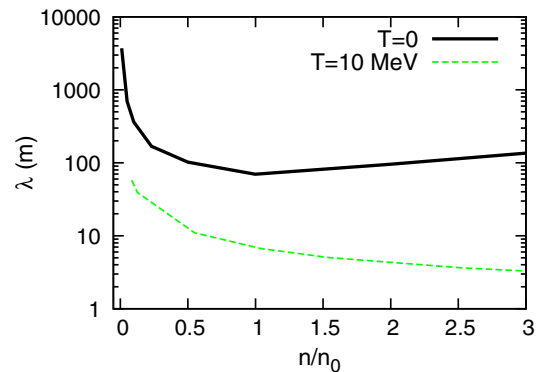


FIG. 7. DM particle mean free path as a function of density (in units of n_0) for two values of temperature, $T = 0$ and $T = 10$ MeV. Effective (naked) nucleon mass has been used in the zero (finite) T calculation.

naked nucleon mass is considered. Incoming energy has been fixed to $\omega = 1.26m_\chi$ for each case. Temperature effects, which are relevant in the early stages of dense star evolution, tend to increase the opacity of nucleon matter to prevent DM nearly free streaming.

In order to qualitatively compare our findings with existing current experiments, we consider generic sensitivities constrained from direct and collider searches. In this part, our aim is to see how our results fit in the global present picture of relativistic scattering of DM coming from a complementary and different scenario.

From our earlier discussion, the scenario we present in our work is meaningful for a χN cross section larger than that of the geometrical cross section $\langle\sigma_{\chi N}\rangle \sim \sigma_0 \simeq \pi R^2 m_n/M \sim 10^{-45} \text{ cm}^2$. Typical constrained values in current experiments are larger than this value. In order to compare strengths, we consider a typical reference value of central baryonic density in the star $n = 2n_0$ and estimate integrated cross sections *per particle*, averaging over the nucleon particle density, as $\langle\sigma_{\chi N}\rangle \simeq \frac{\sigma_{\chi N}/V}{n}$.

Using our set of generic couplings g_{Ns}, g_{Nv} we obtain scalar and vector contributions $\langle\sigma_{s,\chi N}\rangle \sim 10^{-47}$, $\langle\sigma_{v,\chi N}\rangle \sim 10^{-43} \text{ cm}^2$ for masses in the range $m_\chi \sim \text{GeV}$. These results must be considered as an averaged value in momentum space and are consistent with existing collider constraints on D1 and D5 couplings [24,25] at the $m_\chi \sim \text{GeV}$ range derived in the context of EFT. Note that these quoted constraints on collider and direct searches should be however taken with caution since they present some already well-known problems, i.e., (over-) under-estimates and inconsistencies with the thermal relic density for m_χ ranges outside a $m_\chi \sim (170\text{--}500) \text{ GeV}$ range, see the discussion in [33,34]. The energy range that we describe in the relativistically boosted scenario accounts for center-of-mass energies of $\sqrt{s} \lesssim 6 \text{ GeV}$ for DM candidates with $m_\chi \lesssim 5 \text{ GeV}$ scattering target nucleons in a dense nuclear sea. However, as stated in [34], it is also the momentum transfer and mediator mass, M_ϕ , that provide the validity of interpretation of EFT as it must fulfill $q^2 \ll M_\phi^2$.

In the current status of the direct detection DM search in the low mass range region, CDMS [35] and SuperCDMS SNOLAB [36] provide the best limits up to date with a sensitivity of $\sigma_{\chi N} \sim 10^{-41} \text{ cm}^2$ for a limiting value $m_\chi \sim 5 \text{ GeV}$. Below this mass, collider searches can provide better sensitivities than direct searches because the momentum transfer becomes small and the nuclear recoil energy falls below experimental thresholds. We expect, nevertheless, that a more refined model of the hadron structure or the mediators in the interaction will provide a richer contribution to be determined in the future,

as this is far from the present scope of this work. We consider that, despite indirectly, dense astrophysical sites can contribute to probing the low mass region of the DM phase space.

IV. CONCLUSIONS

In summary, we have calculated dark matter scattering cross sections in an environment of dense and hot nucleon matter. We have considered a fermionic DM particle with scalar and vector effective couplings. In this scattering scenario, we have tested a low mass region $m_\chi \lesssim 5 \text{ GeV}$. Examples for this setting are the interiors of neutron stars, where core densities range typically exceed $n/n_0 \gtrsim 1$ and temperatures $T \lesssim 50 \text{ MeV}$. We have included the nuclear medium effects through Fermi-Dirac distributions for the nucleon sector, assuming the amount of DM mass in the star remains tiny at all times. To partially correct for the fact that we consider a point-like interaction, we use monopolar form factors for the hadron structure. We find that the differential and integrated cross sections are greatly affected by the finite density of matter, namely, by the effect of a smaller effective nucleon mass $m_N^* < m_N$. Temperature effects are taken into account with additional detailed balance factors and are found to be important, although to a lesser extent relative to density. The mean free path for a DM particle is found to be larger than the typical values of those found for Standard Model neutrinos with vector-axial couplings. The simplified estimate for the mean free path, $\lambda_\chi \simeq 1/\sigma_{\chi N}n$, lacks the rich dependence on the phase space of the scattering process. In this paper, we show that the diffusive behavior approximation at finite density and temperature in the interior of NS is well grounded and DM can contribute to the energy transport in their interior. While a specific application to proto-neutron stars is deferred to a later paper, here, we have discussed the interest of dense neutron stars to expose the importance of the medium effects in the interaction of ordinary and dark matter.

ACKNOWLEDGMENTS

M. A. P.-G. acknowledges interesting discussions with C. Albertus, R. Lineros, and J. Horvath. This research has been partially supported by University of Salamanca, Grants No. FIS2012-30926 and No. FIS2015-65140, MULTIDARK MINECO projects, and at IAP by the ERC project 267117 (DARK) hosted by Université Pierre et Marie Curie—Paris 6 and at JHU by NSF Grant No. OIA-1124403. M. C. is supported by a fellowship from the Consolider MULTIDARK project and Universidad de Salamanca.

- [1] M. McCullough and M. Fairbairn, *Phys. Rev. D* **81**, 083520 (2010); D. Hooper, D. Spolyar, A. Vallinotto, and N. Y. Gnedin, *Phys. Rev. D* **81**, 103531 (2010).
- [2] W. H. Press and D. N. Spergel, *Astrophys. J.* **296**, 679 (1985).
- [3] A. Peter, Ph.D. Thesis, Princeton University, 2008.
- [4] A. Gould, *Astrophys. J.* **321**, 571 (1987); I. Goldman and S. Nussinov, *Phys. Rev. D* **40**, 3221 (1989); C. Kouvaris, *Phys. Rev. D* **77**, 023006 (2008).
- [5] D. Bauer *et al.*, [arXiv:1310.8327v2](https://arxiv.org/abs/1310.8327v2); M. Klasen, M. Pohl, and G. Sigl, *Prog. Part. Nucl. Phys.* **85**, 1 (2015).
- [6] M. Cirelli, *Pramana* **79**, 1021 (2012).
- [7] I. Lopes and J. Silk, *Science* **330**, 462 (2010).
- [8] C. Kouvaris and P. Tinyakov, *Phys. Rev. D* **83**, 083512 (2011).
- [9] S. D. McDermott, H.-B. Yu, and K. M. Zurek, *Phys. Rev. D* **85**, 023519 (2012).
- [10] J. Bramante, K. Fukushima, and J. Kumar, *Phys. Rev. D* **87**, 055012 (2013).
- [11] M. A. Pérez-García, J. Silk, and J. R. Stone, *Phys. Rev. Lett.* **105**, 141101 (2010).
- [12] M. A. Pérez-García and J. Silk, *Phys. Lett. B* **711**, 6 (2012).
- [13] M. A. Pérez-García, F. Daigne, and J. Silk, *Astrophys. J.* **768**, 145 (2013).
- [14] M. A. Pérez-García and J. Silk, *Phys. Lett. B* **744**, 13 (2015).
- [15] S. Ritz and D. Seckel, *Nucl. Phys.* **B304**, 877 (1988).
- [16] D. Page, J. M. Lattimer, M. Prakash, and A. W. Steiner, *Astrophys. J.* **155**, 623 (2004).
- [17] H. Y. Cheng and C. W. Chiang, *J. High Energy Phys.* **07** (2012) 009.
- [18] A. Alvesa, A. Berlin, S. Profumo, and F. S. Queiroz, *J. High Energy Phys.* **10** (2015) 076.
- [19] M. Cannoni, M. E. Gómez, M. A. Pérez-García, and J. D. Vergados, *Phys. Rev. D* **85**, 115015 (2012).
- [20] B. Bertoni, A. E. Nelson, and S. Reddy, *Phys. Rev. D* **88**, 123505 (2013).
- [21] A. L. Fitzpatrick, W. Haxton, E. Katz, N. Lubbers, and Y. Xu, *J. Cosmol. Astropart. Phys.* **02** (2013) 004.
- [22] J. Goodman, M. Ibe, A. Rajaraman, W. Spherd, T. M. P. Tait, and H. Yu, *Phys. Rev. D* **82**, 116010 (2010).
- [23] K. Cheung, P. Tseng, Y. S. Tsai, and T. Yuan, *J. Cosmol. Astropart. Phys.* **05** (2012) 001.
- [24] G. Aad *et al.*, *Phys. Rev. D* **90**, 012004 (2014); G. Aad *et al.*, *Phys. Rev. D* **91**, 012008 (2015).
- [25] V. Khachatryan *et al.* (CMS Collaboration), *Eur. Phys. J. C* **75**, 235 (2015); *Phys. Lett. B* **755**, 102 (2016).
- [26] M. Bañados, J. Silk, and S. M. West, *Phys. Rev. Lett.* **103**, 111102 (2009).
- [27] S. Reddy, M. Prakash, and J. M. Lattimer, *Phys. Rev. D* **58**, 013009 (1998).
- [28] K. A. Olive *et al.* (Particle Data Group Collaboration), *Chin. Phys. C* **38**, 090001 (2014).
- [29] B. D. Serot and J. D. Walecka, *Advances in Nuclear Physics*, edited by J. W. Negele and E. Vogt (Plenum, New York, 1986).
- [30] C. J. Horowitz and M. A. Pérez-García, *Phys. Rev. C* **68**, 025803 (2003).
- [31] C. J. Horowitz and K. Wehrberger, *Phys. Lett. B* **266**, 236 (1991).
- [32] M. A. Pérez-García, *Eur. Phys. J. A* **44**, 77 (2010).
- [33] Y. Bai, P. J. Fox, and R. Harnik, *J. High Energy Phys.* **12** (2010) 048.
- [34] O. Buchmueller, M. J. Dolan, and C. McCabe, *J. High Energy Phys.* **01** (2014) 025.
- [35] R. Agnese *et al.* (CDMS Collaboration), *Phys. Rev. Lett.* **111**, 251301 (2013).
- [36] R. Agnese *et al.* (SuperCDMS Collaboration), *Phys. Rev. Lett.* **112**, 041302 (2014).